RESPIRATORY MEDICINE

Lecture Notes

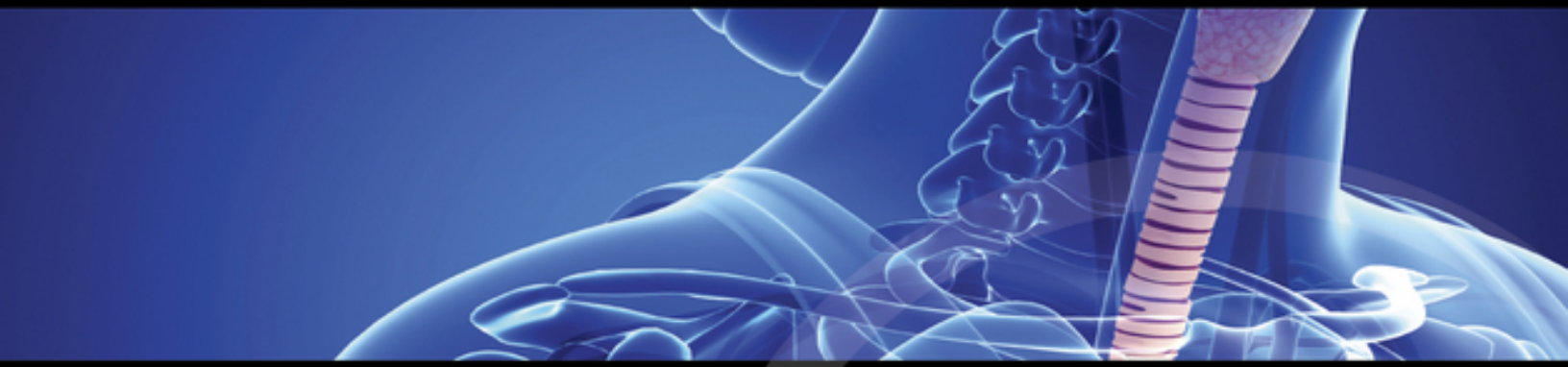

Stephen J. Bourke
Graham P. Burns

9th Edition

with self-test

WILEY Blackwell

Table of Contents

List of Illustrations

when the RQ is 1 versus 0.8. (a) A hypothetical sample of arterial blood. (b) Progressive underventilation. (c) Po_2 lower than can be accounted for by underventilation alone.

Figure 1.9 Blood oxygen and carbon dioxide dissociation curves drawn to the same scale.

Figure 1.10 Distribution of ventilation/perfusion (V/Q) relationships within the lungs. Although the overall V/Q ratio is the same in the two examples shown, the increased spread of V/Q ratios within the diseased lung (b) will result in a lower arterial oxygen tension and content than in the normal lung (a). Arterial Pco_2 will be similar in both cases.

Figure 1.11 Effect of ventilation/perfusion (V/Q) imbalance. (a) Appropriate V/Q. The V/Q ratio is shown diagrammatically on the left. When ventilation is appropriately matched to perfusion in an alveolus or in the lung as a whole, the Pco_2 is about 5.3 kPa (40 mmHg) and the Po_2 is about 12.6 kPa (95 mmHg). The dissociation curves shown in the centre of the diagram describe the relationship between the blood gas tension and the amount of gas carried by the blood. The normal blood gas contents are represented very diagrammatically on the right. (b) Low V/Q. Reduced ventilation relative to blood flow results in a rise in arterial Pco_2 and a fall in Po_2. Reference to the dissociation curves shows that this produces a rise in arterial CO_2 content and a fall in O_2 content. (c) High V/Q. Increased ventilation relative to blood flow results in a fall in Pco_2 and a rise in Po_2. Reference to the dissociation curves shows that this results in a fall in CO_2 content below

the normal level but no increase in O_2 content. In health, the vast majority of alveoli have an appropriate balance of ventilation and perfusion and the arterial blood has a normal CO_2 and O_2 content, as shown in (a). In many disease states, the V/Q ratio varies widely between areas. Such variation always results in a disturbance of blood gas content. The effects of areas of low V/Q are not corrected by areas of high V/Q. The result of mixing blood from areas of low and high V/Q is shown diagrammatically on the extreme right (d). It can be seen that, with respect to CO_2 content, the high content of blood from underventilated areas is balanced by the low content from overventilated areas. However, in the case of O_2, the low content of blood from underventilated areas cannot be compensated for by an equivalent increase in the O_2 content of blood from overventilated areas. *Arterial hypoxaemia is inevitable if there are areas of low V/Q (relative underventilation or overperfusion).*

Chapter 2: History taking and examination

Figure 2.1 Which man has airway obstruction? (Answer at foot of this page.)

Figure 2.2 Clubbing. (a) Normal: the ‘angle’ is shown. (b) Early: the angle is absent. (c) Advanced: the nail shows increased curvature in all directions, the angle is absent, the base of the nail is raised up by spongy tissue and the end of the digit is expanded.

Figure 2.3 Movement of the costal margin. The arrows indicate the direction of movement in normal individuals and in those with airway obstruction (see text). The sign is most easily detected by placing the first and second fingers of each hand in the positions

reduced below the predicted value, but it represents a large part of the FVC. The forced expiratory ratio is >90%. (c) *Obstructive ventilatory defect*. The FEV_1 is much reduced. The rate of airflow is severely reduced, as indicated by the reduced slope of the curve. Note that the forced expiratory time is increased: the patient is still blowing out at 5 seconds. The VC has not been adequately recorded in this case, because the patient did not continue the expiration after 5 seconds; he or she could have expired further. (This is a common technical error). (d) *Severe airway obstruction*. The FEV_1 is about 0.5 l. The FVC is also reduced, but not so strikingly as FEV_1. Forced expiratory ratio is 23%. Very low expiratory flow rate. This pattern of a very brief initial rapid phase followed by a straight line indicating little change in maximal flow rate with change in lung volume is sometimes thought to be indicative of severe emphysema, although identical results can be observed in severe asthma. (e) *Airway obstruction and bronchial hyperreactivity*. Five expirations have been made. FEV_1 and FVC become lower with each expiration. Patient with asthma. These features suggest poor control of asthma and liability to severe attacks. (f) *A non-maximal expiration*. Compare with (a). In a true forced expiration, the steepest part of the curve always occurs at the beginning of expiration, which is not the case here. A falsely low FEV_1 and forced expiratory ratio are obtained. Usually, the patient has not understood what is required or is unable to coordinate his or her actions. Some patients wish to appear worse than they really are. This pattern is unlikely to be mistaken for a true forced expiration because of its shape and because it cannot be

reproduced repeatedly. (g) *Escape of air* from the nose or lips during expiration. (h) *Inability to perform the manoeuvre*. Five attempts have been made. In some, the patient has breathed in and out. Other attempts are either not maximal forced expirations or are unfinished. Bizarre patterns such as this are often seen in patients with psychogenic breathlessness or in the elderly. Even with poor cooperation, it is often possible to obtain useful information. In the example shown, significant airway obstruction can be excluded because of the steep slope of at least two of the expirations, which follow an identical course and show appropriate curvature (dotted line), and the FVC can be estimated as not less than 3.2 l. The pattern seen in large airway obstruction is shown in Figure 3.5 and 3.6.

Figure 3.5 Large (central) airway obstruction. Typical tracing obtained with a spirometer. The subject has made three maximal forced expirations. Each shows a striking straight section, which then changes relatively abruptly, at about the same volume, to follow the expected curve of the forced expiratory spirogram. The straight section is not as reproducible as a normal spirogram. A 'family' of similar tracings is thus obtained, each with straight and curved sections. Explanation: over the straight section, flow is limited by the fixed intrathoracic localised obstruction. This is little influenced by lung recoil, so the critical flow is similar during expiration and the spirogram appears straight. A lung volume is eventually reached at which maximum flow is even lower than that permitted by the central obstruction. The ordinary forced expiratory spirogram is described after this point. In the example shown, there must be an element of diffuse airway

obstruction, as forced expiratory time is somewhat prolonged (see Figure 3.2c).

Figure 3.6 Further flow/volume loops. The dotted outline represents a typical normal loop. The small graphs show the appearances of a forced expiration on a spirometer (as in Figure 3.2). (a) Demonstration of maximum flow. A normal individual makes an unhurried expiration from full inspiration and then, about halfway through the VC, makes a maximal expiratory effort (Ef). The flow/volume tracing rejoins the maximum flow/volume curve, which describes the maximum flow that can be achieved at that lung volume. Also shown in is the flow/volume loop of typical tidal breathing. At the resting lung volume, an abundant reserve of both inspiratory and expiratory flow is available. (b) Moderate airway obstruction (asthma or COPD). Maximum expiratory flow is reduced. The declining portion of the expiratory limb has a characteristic curvilinearity. Inspiration is less severely affected. (c) Very severe airway obstruction. Maximum expiratory flow is very severely reduced. There is a brief peak, followed by an abrupt fall in flow rate (probably caused by some airway closure), after which flow falls very slowly. Also shown in is a loop representing quiet tidal breathing. It is clear that every expiration is limited by maximum flow. Expiratory wheezing or pursed-lip breathing would be expected. The tidal loop has been obliged to move to the left, as the patient is ventilating at a higher lung volume. This has obviated, to some degree, the airway narrowing, but adds to the work of breathing and contributes to the sensation of breathlessness (see Chapter 1). (d) Intrathoracic large airway obstruction. Here the peak inspiratory and expiratory flows have been truncated in a characteristic pattern.

Intrathoracic lesions (e.g. tracheal compression by a mediastinal tumour) have a more pronounced effect on the expiratory limb than the inspiratory limb. (e) Extrathoracic obstruction (e.g. tracheal compression by a goitre in the neck). This results in inspiratory collapse of the airway below the obstruction (but still outside the thorax), attenuating maximum inspiratory flow rate to a greater degree than maximum expiratory flow rate.

Figure 3.3 Measurement of PEF. The subject takes a *full inspiration*, applies their lips to the mouthpiece and makes a sudden maximal expiratory blast. A piston is pushed down the inside of the cylinder, progressively exposing a slot in the top, until a position of rest is reached. The position of the piston is indicated by a marker and PEF is read from a scale. It is customary to take the best of three properly performed attempts as the PEF.

Figure 3.4 Flow/volume loop. Airflow is represented on the vertical axis and lung volume on the horizontal axis. The line Z–Z represents zero flow. Expiratory flow appears above the line; inspiratory flow, below. PEF, peak expiratory flow; RV, residual volume; TLC, total lung capacity.

Figure 3.7 Relative effects on expiratory and inspiratory flow of intra- and extrathoracic large airway obstruction. Top: Large airway obstruction within the thorax. (a) Positive intrathoracic (alveolar) pressure generated during expiration acts to compress the airway and further narrow the point of obstruction. (b) Negative intrathoracic pressure during inspiration acts to reduce narrowing at the point of obstruction. Therefore, in large airway obstruction within the thorax, expiratory flow is

diminished to a greater degree than inspiratory flow (see Figure 3.6d). Bottom: Large airway obstruction outside the thorax. (c) Positive pressure within the airway during expiration in relation to atmospheric ('zero') pressure outside acts to reduce narrowing at the point of obstruction. (d) Negative pressure within the airway during inspiration acts to compress the airway and further narrow the point of obstruction. Therefore, in large airway obstruction outside the thorax, inspiratory flow is diminished to a greater degree than expiratory flow (see Figure 3.6e).

Figure 3.8 Measurement of transfer factor by the single-breath method. Schematic representation of the helium and carbon monoxide concentrations in the inspired mixture and in alveolar air during breath holding.

Figure 3.9 Bicarbonate isopleths (diagonal lines; the bicarbonate level is constant along the lines). It can be seen that, if the bicarbonate level and Pco_2 are known, the pH can be calculated. Indeed, if any two of the three values of bicarbonate, pH and Pco_2 are known then the other value can be calculated. These values are yoked together. A change in ventilation will move the arterial point up or down an isopleth as shown, changing pH (bicarbonate level does not change). A pure metabolic disturbance (before any respiratory response) changes the bicarbonate level, moving from one bicarbonate isopleth to another and changing pH.

Figure 3.10 Acid/base disturbances. The oval indicates the normal position, the shaded areas indicate the directions of observed 'pure' or uncomplicated disturbances of acid/base balance. Bicarbonate levels are omitted for clarity. Letters (a)–

(d) are referred to in the section on mixed disturbances.

Chapter 4: Radiology of the chest

Figure 4.1 Diagram of chest X-ray (PA view). The right hemidiaphragm is 1–3 cm higher than the left (a) and on full inspiration is intersected by the shadow of the anterior part of the sixth rib (b). The trachea (c) is vertical and central. The horizontal fissure (d) is found in the position shown and should be truly horizontal. It is a very valuable marker of a change in volume of any part of the right lung but is not always visible. The left border of the cardiac shadow comprises: (e) aorta, (f) pulmonary artery, (g) concavity overlying the left atrial appendage and (h) left ventricle. The right border of the cardiac shadow normally overlies the right atrium (i) and sits above that of the superior vena cava.

Figure 4.2 Diagram of chest X-ray (lateral view). (a) Trachea. (b) Oblique fissure. (c) Horizontal fissure. It is useful to note that in a normal lateral view, the radiodensity of the lung field above and in front of the cardiac shadow is about the same as that below and behind (x). Ao, aorta.

Figure 4.3 Radiographic patterns of lobar collapse. Collapsed lobes occupy a surprisingly small volume and are commonly overlooked on the chest X-ray. Helpful information may be provided by the position of the trachea, the hilar vascular shadows and the horizontal fissure. LLL, left lower lobe; LUL, left upper lobe; RLL, right lower lobe; RML, right middle lobe; RUL, right upper lobe.

Figure 4.4 The left lower lobe has collapsed medially and posteriorly and appears as a dense white

triangular area behind the heart, close to the mediastinum. The remainder of the left lung appears hyperlucent because of compensatory expansion. Bronchoscopy showed an adenocarcinoma occluding the left lower lobe bronchus.

Figure 4.5 Left lung collapse. There is complete opacification of the left hemithorax, with a shift of the mediastinum to the left. Bronchoscopy showed a small-cell carcinoma occluding the left main bronchus.

Figure 4.6 The silhouette sign, showing abnormal lung shadowing in the left lower zone. Where the sharp outline of mediastinal structures or diaphragm is lost because of normal lung opacification, it can be concluded that the shadow is immediately adjacent to the structure (and vice versa). In example (a), the shadow must be anterior and next to the heart as the sharp outline of the heart is lost. In (b), it must be posterior, as the heart outline is preserved.

Figure 4.7 Chest X-ray showing multiple partially calcified rounded masses in both lungs, caused by benign chondromas.

Figure 4.8 A cavitating lesion in the left upper lobe. A cavity appears as an area of radiolucency (black) within an opacity (white). Sputum cytology showed cells from a squamous carcinoma. CT showed left hilar and subcarinal lymphadenopathy.

Figure 4.9 Mediastinal masses. Diagram of lateral view of the chest, indicating the sites favoured by some of the more common mediastinal masses.

Figure 4.10 Mediastinal structures; principal blood vessels and airways. Top: heart and major blood vessels, showing the aorta curling over the

bifurcation of the pulmonary trunk into left and right pulmonary arteries (arrows). The horizontal lines (a)–(d) indicate the levels of the CT sections illustrated in Figure 4.11. 1, right brachiocephalic vein; 2, left brachiocephalic vein; 3, innominate or brachiocephalic artery; 4, left common carotid artery; 5, left subclavian artery. Bottom: structures with the heart removed. The aorta curls over the left main bronchus, which lies behind the left pulmonary artery. Pulmonary arteries are shown shaded, pulmonary veins are shown unshaded and bronchi are shown striped. In general, the arteries loop downwards, like a handlebar moustache. Veins radiate towards a lower common destination: the left atrium. The veins are applied to the fronts of the arteries and bronchi and take a slightly different path to the respective lung segments. On the right, the order of structures from front to back is vein–artery–bronchus; on the left, the pulmonary artery loops over the left upper lobe bronchus and descends behind, so that the order is vein–bronchus–artery.

Figure 4.11 Principal mediastinal structures on CT. Sections (a)–(d) are at levels (a)–(d) in Figure 4.10. The sections should be regarded as being viewed from below **(i.e. the left of the thorax is on the right of the figure)**. (a) *Section above the aortic arch*. Many large vessels and an anterior sausage shape are seen; the trachea has not bifurcated (black circle). Numerals refer to Figure 4.10 and its legend. (b) *Section at the level of the aortic arch*. A large oblique sausage shape representing the aortic arch is seen (ao). oes, oesophagus (visible in all of the sections); svc, superior vena cava. (c) *Section below the aortic arch*. Both ascending (aao) and descending (dao) aortas are visible. The trachea is bifurcating

hobby and one of his budgerigars had died recently. The clinical diagnosis of psittacosis was subsequently confirmed by serology tests. He was treated with intravenous fluids, oxygen and tetracycline, and recovered fully.

Figure 6.4 Pneumococcal pneumonia. This 70-year-old man was admitted to hospital with severe community-acquired pneumonia. He was confused, with a fever of 39 °C, respiratory rate 32/min, blood pressure 90/50 mmHg and urea 22 mmol/l. His CURB-65 score was 5, indicating severe pneumonia. He was admitted to the ITU but died despite treatment with antibiotics, mechanical ventilation and full supportive care. Blood cultures isolated *Streptococcus pneumoniae*. In the UK, about 1 in 1000 of the population is admitted to hospital each year with community-acquired pneumonia and about 18% of these patients die.

Figure 6.5 Pneumocystis pneumonia (PCP). This 28-year-old woman, who was an intravenous drug misuser, presented with fever, dyspnoea and hypoxaemia (Po_2 8.2 kPa (62 mmHg)). The chest X-ray shows diffuse bilateral perihilar and lower zone shadowing. HIV antibody test was positive and CD4 T-lymphocyte count was 100/mm^3 (normal 600–1600/mm^3). Induced sputum was positive for *Pneumocystis jirovecii* on immunofluorescent monoclonal antibody testing. The patient responded fully to high-dose intravenous co-trimoxazole, prednisolone and oxygen, and she was then commenced on long-term secondary prophylaxis with oral co-trimoxazole 3 days/week. When her PCP had been fully treated, highly active antiretroviral therapy (HAART) was started.

Chapter 7: Tuberculosis

apical membrane, where it functions as a cAMP-dependent chloride channel. Class I mutations disrupt synthesis of CFTR. These include nonsense and frameshift mutations, which lead to premature termination codons (PTCs) and lack of protein production. Class II mutations result in misfolded CFTR, whcih is then degraded in the endoplasmic reticulum. In class III mutations, CFTR reaches the apical membrane but is not activated. Class IV mutations result in reduced CFTR conductance. In class V mutations, there is reduced synthesis of normal CFTR and therefore reduced CFTR function at the cell membrane. CFTR has additional regulatory effects on epithelial sodium channels (ENaCs) and on calcium-activated chloride channels (CaCCs). Small-molecule therapies are now becoming available, which overcome some of the molecular defects. Ivacaftor is a potentiator that improves CFTR function at the cell surface in patients with class III mutations (e.g. G551D). Lumacaftor is a corrector that improves the trafficking of mutant CFTR through the cell in patients with the ΔF508 mutation. Ataluren allows ribosomes to read through PTCs in some class I mutations.

Figure 9.2 Clinical features of cystic fibrosis. Cystic fibrosis is a multisystem disease resulting from mutations of the gene that codes for CFTR, which functions as a chloride channel on epithelial membranes. Failure of chloride conductance results in abnormal secretions and organ damage in the respiratory, pancreatic, hepatobiliary, gastrointestinal and reproductive tracts.

Figure 9.3 Chest X-ray of this 37-year-old man with cystic fibrosis shows hyperinflation, peribronchial thickening, cystic bronchiectasis and perihilar

fibrosis. A Portacath central venous system is in place, with the access port situated subcutaneously in the left lower chest. He had chronic *Pseudomonas aeruginosa* infection and received about three courses of intravenous ceftazidime and tobramycin at home each year. His FEV_1 was 1.5 l (42% of predicted) and his general condition and lung function had remained stable over 5 years on treatment including long-term nebulised colistin, nebulised dornase alpha (DNase), physiotherapy and nutritional supplements.

Figure 9.4 Chest X-ray of this 23-year-old man with cystic fibrosis shows the typical appearance of 'cepacia syndrome' with fulminant bilateral necrotising pneumonia. He had acquired *Burkholderia cenocepacia* infection 7 years previously during an outbreak of infection among patients with cystic fibrosis attending a holiday camp. His lung function showed an accelerated rate of decline in the years after infection and he then developed a severe exacerbation that failed to respond to treatment and progressed to a fatal fulminant pneumonia over a 2-week period. Patients with cystic fibrosis are advised not to have contact with one other in order to avoid transmission of infections.

Figure 9.5 This 31-year-old woman with cystic fibrosis was admitted to hospital complaining of abdominal distension, colicky pain and constipation. A mass of inspissated faecal material was palpable in the right iliac fossa. Erect abdominal X-ray (after taking Gastrografin) shows distended loops of small bowel, containing multiple fluid levels. A diagnosis of meconium ileus equivalent (distal intestinal obstruction syndrome) was made and she was treated

Figure 10.5 Example of a spacer device for use with MDIs. This allows the patient to inhale after discharge of the aerosol. The Volumatic (Allen and Hanbury) is a large-volumed device designed to allow free dispersal of the discharged material, so that a high proportion of it forms particles small enough to be inhaled. It also allows large doses of aerosol to be inhaled relatively efficiently (see text). cr, canister of pressurised aerosol; e, expiratory port; v, valve (closes on expiration).

Figure 10.6 Examples of dry-powder inhalers. (a) Turbohaler. The inhaler is shown with the cover removed, the mouthpiece to the left. Up to 200 doses of the powdered drug are stored in a reservoir, through which the air channel passes. A dose of the dry powder is rotated into the air channel by turning the distal section (arrow). The number of doses remaining is indicated in a small window (W). (b) Accuhaler. The inhaler is opened by pushing the thumb grip (T) right around until it clicks. The inhaler is shown open. Sliding the lever (L) around as far as it will go pierces an individual blister and places a dose of the drug in the mouthpiece (M). There is a counter (C) indicating how many doses are left. (c) Genuair. When the button is pressed and released, the control window changes to green, indicating the drug is ready to be inhaled. Inhalation changes the control window to red and locks the inhaler out, preventing further inhalation until the button is pressed again.

Figure 10.7 Nebuliser treatment. (a) Diagram of typical nebulisation mechanism. (b) Nebuliser mask for administration of high-dose bronchodilator (see text).